Full length article

Probing the frequency-dependent elastic moduli of lattice materials

T. Mukhopadhyay [a, *], S. Adhikari [b], A. Alu [c]

[a] Department of Engineering Science, University of Oxford, Oxford, UK
[b] College of Engineering, Swansea University, Swansea, UK
[c] Cockrell School of Engineering, The University of Texas at Austin, Austin, USA

ARTICLE INFO

ABSTRACT

An insightful mechanics-based concept is developed for probing the frequency-dependence in in-plane elastic moduli of microstructured lattice materials. Closed-form expressions for the complex elastic moduli are derived as a function of frequency by employing the dynamic stiffness matrix of beam elements, which can exactly capture the sub-wavelength scale dynamics. It is observed that the two Poisson's ratios are not dependent on the frequency of vibration, while the amplitude of two Young's moduli and shear modulus increase significantly with the increase of frequency. The variation of frequency-dependent phase of the complex elastic moduli is studied in terms of damping factors of the intrinsic material. The tunable frequency-dependent behaviour of elastic moduli in lattice materials could be exploited in the pseudo-static design of advanced engineering structures which are often operated in a vibrating environment. The generic concepts presented in this paper introduce new exploitable dimensions in the research of engineered materials for potential applications in various vibrating devices and structures across different length-scales.

© 2018 Acta Materialia Inc. Published by Elsevier Ltd. All rights reserved.

1. Introduction

Engineered lattice materials or mechanical metamaterials are artificial microstructures with bulk mechanical properties defined by their structural configuration along with the intrinsic material properties of the constituent members. The global mechanical properties can be engineered by intelligently identifying the material microstructures of metamaterials. This novel class of structural materials with tailorable global mechanical properties (like equivalent elastic moduli, buckling, vibration and wave propagation characteristics) have tremendous potential applications for future aerospace, civil and mechanical structures. Development of such application-specific engineered materials have received immense attention from the concerned scientific community in last few years after the recent advancement in 3D printing technology [2,4–6,8,13,19,22,24,26,29,30,51,55,58,60,62]. Fascinating properties such as extremely lightweight, negative elastic moduli, negative mass density, unbounded thermal expansion, pentamode material characteristic (meta-fluids) can be obtained by cognitively identifying the material microstructure. For example, if the cell angle θ in Fig. 1 (b) becomes negative, the cellular structure shows auxetic properties i.e. negative Poisson's ratio [1,10,18,39,43]. Natural materials can not exhibit such unusual properties, which can have various favourable applications in wide range of systems.

Metamaterials comprise periodic structural forms in two and three dimensional spaces. For eliminating the requirement of an intricate microscale finite element model for metamaterials as a constituent part of complex large-scale structural systems, such lattice metamaterials are normally modelled as a continuous solid medium with an effective elastic moduli throughout the entire domain [34,41,47,56]. The most prominent approach of analysing metamaterials is to consider an appropriate unit cell that can represent the entire material micro-structure [17,25,36,64]. Two dimensional hexagonal honeycomb-like metamaterials with tailorable elastic moduli have been widely investigated [11,14,27,33,50,57,61,63]. Such hexagonal lattices of natural and artificial nature can be identified across different length-scales (nano to macro) in auxetic and non-auxetic forms. The basic mechanics of deformation for the lattices being scale-independent, the formulations developed in this context are normally applicable for a wide range of materials and structural forms. Experimental and finite element studies have been reported for impact, crushing, elastic moduli and other mechanical responses of normal and foam-filled honeycombs considering manufacturing irregularities

---

* Corresponding author.
E-mail address: tanmoy.mukhopadhyay@eng.ox.ac.uk (T. Mukhopadhyay).
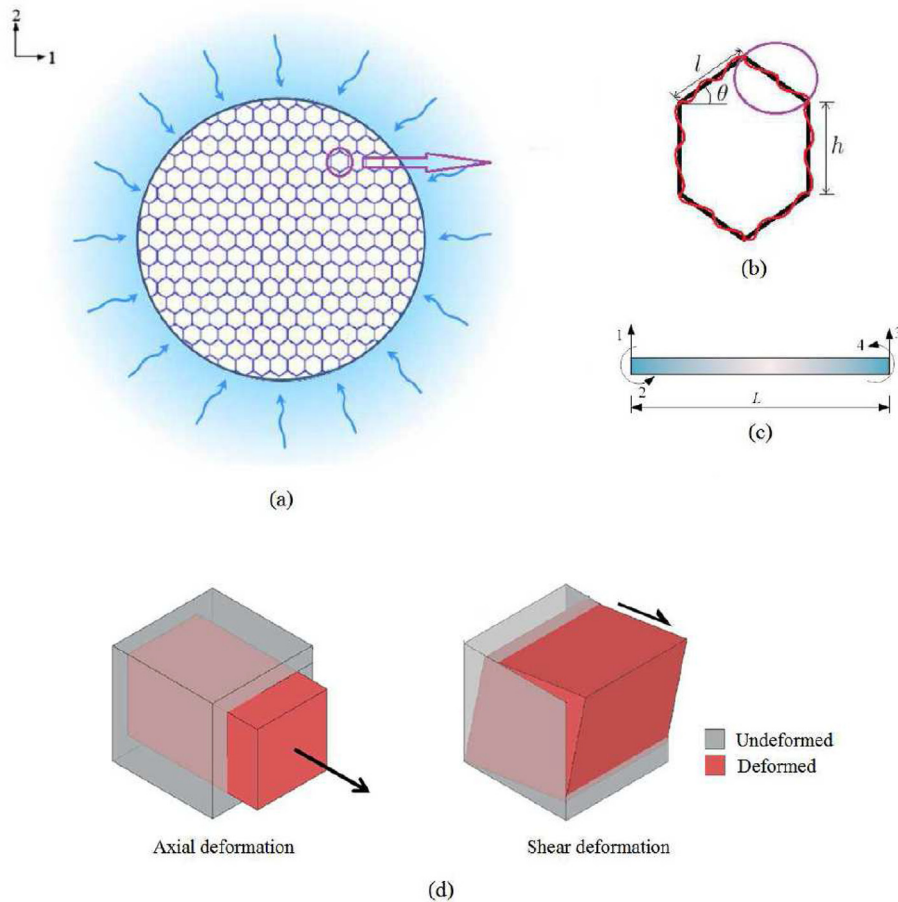
Fig. 1. (a) Typical representation of a hexagonal cellular structure in a dynamic environment (such as the honeycomb as part of a host structure experiencing wave propagation, vibrating structural component etc.). The curved black arrows are symbolically used to indicate propagation of wave (b) One hexagonal unit cell under dynamic environment (c) A dynamic Euler-Bernoulli beam element for the bending vibration of a damped beam with length L (It has two nodes and four degrees of freedom consisting of the transverse deformation and the rotation at the two nodes. The displacement field within the element is expressed by complex frequency dependent shape functions.) (d) Typical representation of axial and shear deformation in materials along with respective applied stresses.

and defects [16,23,28,31,40,42,44,48,49,54]. Honeycombs and other forms of metamaterials are often intended to be utilized in vibrating structures such as sandwich panels used in aircraft structures. Dynamic homogenization of metamaterials have been reported in various recent papers [38,52]. Hexagonal lattice-like structural form being a predominant material structure at nano-scale (such as graphene, hBN etc [32,45,46]), analysis of vibrating nanostructures are quite relevant to various applications at nano-scale. Besides that recent development in the field of metamaterials have prompted its use as advanced materials in aircraft and other machineries that experience vibration during operation. Analytical expressions for equivalent elastic moduli of cellular metamaterials proposed hitherto are based on static deformation only. It is important to investigate the elastic properties of such cellular metamaterials in a dynamic environment.

For relative low-frequency vibrations, the length of each unit cell will be significantly smaller than the wave-lengths of the global vibration modes. As a result, each unit cell would effectively behave as a sub-wavelength scale resonator. Several exciting and unusual bulk properties of metamaterials have been reported exploiting sub-wavelength scale resonators [21]. These include negative effective elastic modulus [12], negative density (or mass) [59], or

both [7], anisotropy in the effective mass or density [20,53], and non-reciprocal response [15,37]. Theoretically, cellular meta-materials undergoing dynamic forces can also show such unusual behaviour due to the sub-wavelength scale resonator. However, this has not been widely reported mainly due to the difficulties in properly modelling hexagonal unit cells as sub-wavelength scale resonators. In principle, this is possible using very fine finite element discretisations of the individual beam elements in a unit cell. Such an approach will be purely numerical (involving computationally intensive simulations) and will not give the necessary physical insights provided by closed-form expressions. Motivated by this need, the present paper proposes a novel approach based on the dynamic stiffness method [3]. This approach is valid for steady-state dynamics under harmonic excitations. Using this idea, an analytical formulation is developed to investigate the frequency dependence for the elastic moduli of metamaterials rigorously.

We aim to demonstrate the dynamic stiffness based framework for frequency dependent elastic moduli considering two dimensional hexagonal metamaterials in this paper. The dynamic stiffness matrix of a generic beam element is derived first, wherein all the elements of the dynamic stiffness matrix are complex in nature and

dependent on the frequency. Based on the principle of structural mechanics, closed-form expressions for the frequency-dependent elastic moduli of the cellular structure are derived using the dynamic stiffness elements of a beam. This article is organized hereafter as follows: the closed-form expressions of frequency dependent elastic moduli of hexagonal lattices are furnished in section 2 (the detail derivation of the dynamic stiffness matrix for a single beam element and the expressions for elastic moduli of lattice metamaterials are provided in the supplementary material); results of the frequency dependent elastic moduli are presented in section 3 considering different structural and geometric parameters; a brief summary of the results along with their importance and prospective applications in the field of metamaterials are discussed in section 4; and finally, section 5 provides concluding remarks and outlook of the present article.

2. Frequency-dependent elastic moduli

2.1. The dynamic stiffness matrix

Dynamic motion of the overall cellular structure corresponds to vibration of individual beams which constitute each hexagonal unit cells. A representative pictorial depiction of the beam is shown in Fig. 1(c). One typical honeycomb unit cell under dynamic environment is shown in Fig. 1(b), wherein a vibrating mode of each constituent members is symbolically shown. If external forces are applied to such a vibrating honeycomb, the members will deform following a different rule. Thus the effective elastic moduli of the entire lattice will be different from conventional static elastic moduli. Aim of the present article is to capture the effect of vibration in the effective elastic moduli of hexagonal lattices based on dynamic stiffness method [9,35]. Some of the key features of this method are discussed in the following paragraph.

The mass distribution of the elements in dynamic stiffness method is treated in an exact manner for deriving the element dynamic stiffness matrix. The dynamic stiffness matrix of one-dimensional structural elements, taking into account the effects of flexure, torsion, axial and shear deformation, and damping, is exactly determinable, which, in turn, enables the exact vibration analysis by an inversion of the global dynamic stiffness matrix. The method does not employ eigenfunction expansions and, consequently, a major step of the traditional finite element analysis, namely, the determination of natural frequencies and mode shapes, is eliminated which automatically avoids the errors due to series truncation. Since modal expansion is not employed, ad hoc assumptions concerning the damping matrix being proportional to the mass and/or stiffness are not necessary. The method is essentially a frequency-domain approach suitable for steady state harmonic or stationary random excitation problems. The static stiffness matrix and the consistent mass matrix appear as the first two terms in the Taylor expansion of the dynamic stiffness matrix in the frequency parameter.

The overall elastic moduli of the lattice depends on the bending deformation of the individual beams within a unit cell (Fig. 1(b)). When dynamic equivalent elastic moduli are considered, one needs to establish a dynamic equilibrium within the unit cell. The central idea of this work is to exploit the dynamic stiffness matrix of the beam for this purpose. Therefore, the dynamic stiffness matrix of a single beam element is derived first. Next the expressions of frequency dependent elastic moduli of the lattice metamaterial are developed based on the elements of the dynamic stiffness matrix of

a single beam. The equation of motion of free vibration of a damped beam can be expressed as

$$EI\frac{\partial^4 V(x,t)}{\partial x^4} + c_1\frac{\partial^5 V(x,t)}{\partial x^4 \partial t} + m\frac{\partial^2 V(x,t)}{\partial t^2} + c_2\frac{\partial V(x,t)}{\partial t} = 0 \tag{1}$$

It is assumed that the behaviour of the beam follows the Euler-Bernoulli hypotheses. In the above equation EI is the bending rigidity, m is mass per unit length, c_1 is the strain-rate-dependent viscous damping coefficient, c_2 is the velocity-dependent viscous damping coefficient and $V(x,t)$ is the transverse displacement. The length of the beam is L and x is the distance along the length.

When frequency dependent excitation is considered, the beams representing the elements of the lattice undergo dynamic deformation. In Fig. 1(c) we show a finite element representing dynamics of an Euler-Bernoulli beam. The four degrees of freedom correspond to the transverse deformation and the rotation at the two nodes. The dynamic deformation within the beam is interpolated using the shape function and the nodal deformation corresponding to each degrees of freedom. As the deformation is frequency dependent, at any point inside the beam it can be expressed as

$$v(x,\omega) = N_1(x,\omega)\widehat{v}_1(\omega) + N_2(x,\omega)\widehat{v}_2(\omega)N_3(x,\omega)\widehat{v}_3(\omega) \\ + N_4(x,\omega)\widehat{v}_4(\omega), \quad 0 \le x \le L \tag{2}$$

Here $v(x,\omega)$ is the Fourier transform of $V(x,t)$, ω is the excitation frequency, $N_j(x,\omega)$ and $\widehat{v}_j(\omega), j = 1,\cdots,4$ are the shape functions and nodal deformation corresponding to the four degrees of freedom shown in Fig. 1(c) (see the supplementary material for detailed derivations). A crucial difference between the displacement expression in equation (2) and the conventional finite element approach is the use of frequency dependent shape functions. The four shape functions appearing in equation (2) are shown in Fig. 2. It can be seen that the shape functions change not only along the length of the beam but also along the frequency. This allows the displacement field to adapt with changes in the frequency without increasing the degrees of freedom. This in turn enables us to establish a dynamic equilibrium within a unit cell in a simplified manner, leading to the closed-form expressions of the equivalent elastic moduli as discussed next.
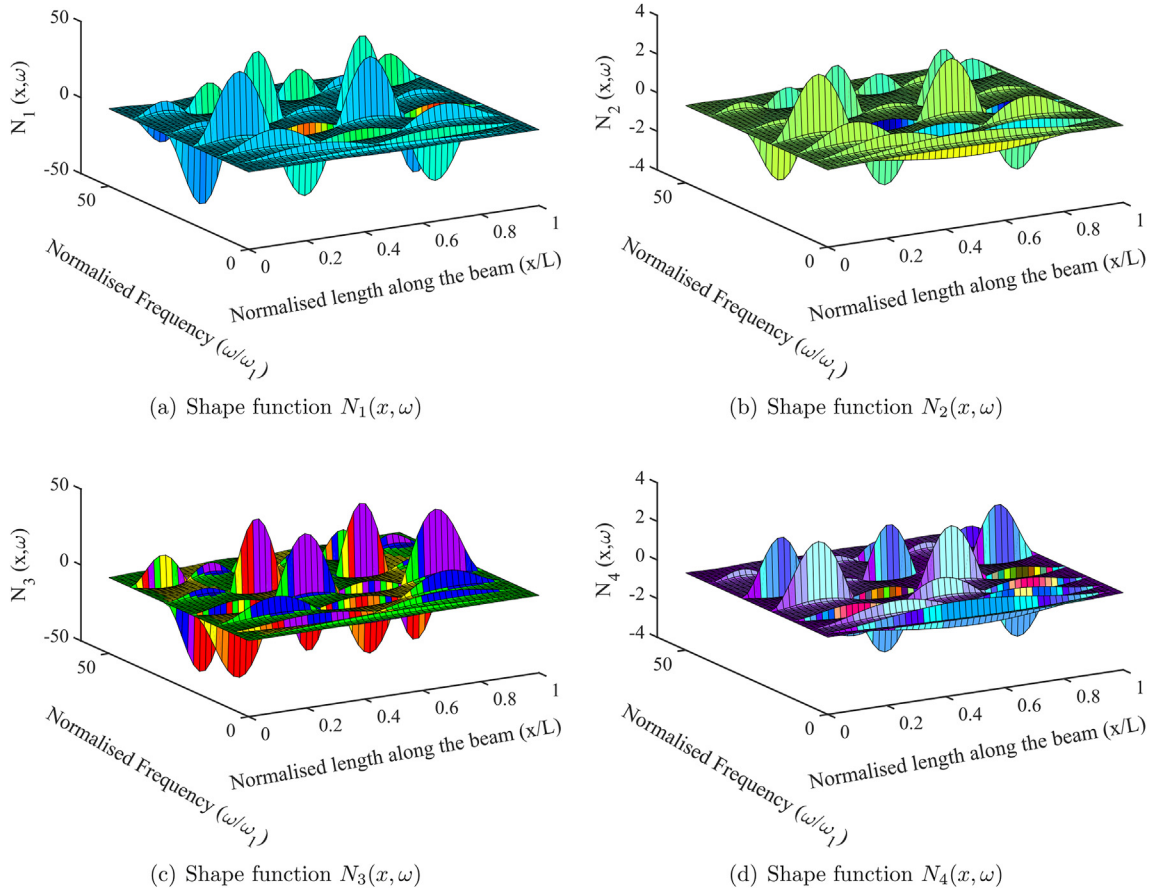
From the equation of motion, the dynamic stiffness matrix of a single beam element can be derived in a closed form as:

$$\mathbf{D}(\omega) = \frac{EIb}{(cC-1)}\begin{bmatrix} -b^2(cS+Cs) & -sbS & b^2(S+s) & -b(C-c) \\ -sbS & -Cs+cS & b(C-c) & -S+s \\ b^2(S+s) & b(C-c) & -b^2(cS+Cs) & sbS \\ -b(C-c) & -S+s & sbS & -Cs+cS \end{bmatrix} \tag{3}$$

where

$$C = \cosh(bL), c = \cos(bL), S = \sinh(bL), s = \sin(bL) \quad \text{and}$$

$$b^4 = \frac{m\omega^2(1-\mathrm{i}\zeta_m/\omega)}{EI(1+\mathrm{i}\omega\zeta_k)} \tag{4}$$

Here $\mathrm{i} = \sqrt{-1}$ and the quantities ζ_k and ζ_m are stiffness and mass proportional damping factors and they are given by

(a) Shape function $N_1(x, \omega)$

(b) Shape function $N_2(x, \omega)$

(c) Shape function $N_3(x, \omega)$

(d) Shape function $N_4(x, \omega)$

Fig. 2. Dynamic shape functions along the length of the beam as a function of frequency. No damping is considered for this illustration. The frequency axis is normalised with the first natural frequency of a pinned-pinned beam.

$$\zeta_k = \frac{c_1}{EI} \quad \text{and} \quad \zeta_m = \frac{c_2}{m} \tag{5}$$

The elements of this matrix are frequency dependent complex quantities because b is a function of ω and the damping factors. Detail derivation of the dynamic stiffness matrix is provided in the supplementary material. For the purpose of deriving the expressions for the lattice metamaterial, the dynamic stiffness matrix (refer to equation (3)) is written in the following form for notational convenience

$$\mathbf{D}(\omega) = [D_{ij}], \quad \text{where} \quad i, j \in [1, 2, \ldots 4] \tag{6}$$

2.2. Expressions of the frequency-dependent elastic moduli

Considering only the static deformation of a unit cell, equivalent elastic moduli of the hexagonal cellular materials were obtained (refer to equations 25−29 of the supplementary material) [17]. A key interest in this section is to obtain equivalent expressions of such lattices when harmonic forcing is considered. The central idea behind the proposed derivation is to exploit the physical interpretation of the elements of the dynamic stiffness matrix, as

discussed in the preceding paragraphs. Using equation (3), the analytical expressions of the frequency dependent in-plane elastic moduli of the hexagonal lattice are obtained. Based on the concept of a unit cell based approach, one hexagonal unit is analysed to derive the expressions of in-plane elastic moduli of the lattice material as follows (refer to the supplementary material for details):

$$
\begin{aligned}
E_1(\omega) &= \frac{D_{33} l \cos \theta}{(h + l \sin \theta) \bar{b} \sin^2 \theta} \\
&= \frac{E t^3 l \cos \theta b^3 (\cos(bl) \sinh(bl) + \cosh(bl) \sin(bl))}{12(h + l \sin \theta) \sin^2 \theta (1 - \cos(bl) \cosh(bl))}
\end{aligned}
\tag{7}
$$

$$
\begin{aligned}
E_2(\omega) &= \frac{D_{33} (h + l \sin \theta)}{l \bar{b} \cos^3 \theta} \\
&= \frac{E t^3 (h + l \sin \theta) b^3 (\cos(bl) \sinh(bl) + \cosh(bl) \sin(bl))}{12 \cos^3 \theta (1 - \cos(bl) \cosh(bl))}
\end{aligned}
\tag{8}
$$

$$G_{12}(\omega) = \frac{(h+l\sin\theta)}{2l\overline{b}\cos\theta} \cdot \frac{1}{\left(-\dfrac{h^2}{4lD_{43}^s} + \dfrac{2}{\left(D_{33}^v - \dfrac{(D_{34}^v)^2}{D_{44}^v}\right)}\right)}$$

$$= \frac{Et^3(h+l\sin\theta)b^3\sin(bl)\sinh(bl)(1+\cos(bh/2)\cosh(bh/2))}{6l\cos\theta\left[h^2b(1-\cos(bl)\cosh(bl))(1+\cos(bh/2)\cosh(bh/2)) + 8l\sin(bl)\sinh(bl)(\cosh(bh/2)\sin(bh/2) - \sinh(bh/2)\cos(bh/2))\right]}$$

$$\tag{9}$$

$$\nu_{12} = \frac{\cos^2\theta}{(h+l\sin\theta)\sin\theta} \tag{10}$$

$$\nu_{21} = \frac{(h+l\sin\theta)\sin\theta}{\cos^2\theta} \tag{11}$$

The expression of b is provided in equation (4); E is the intrinsic elastic modulus of the honeycomb material and t is the thickness of honeycomb wall; h, l and θ are the length of cell walls and cell angle as shown in Fig. 1(b). Detailed derivation of the above expressions is provided in the supplementary material.

The developed closed-form expressions of the frequency-dependent elastic moduli can provide a clear understanding of the stiffness and mass contribution in the dynamic regime. It can be noted that the geometric parameters (such as h, l, t and θ) and the intrinsic Young's modulus (b is a function of E) are the components of

2.2.2. Remark 2: the static limit

From the expressions obtained in the preceding subsections, it is evident that E_1, E_2 and G_{12} are functions of the frequency, damping parameters, geometric dimensions of the hexagonal lattice and the intrinsic material property of the material. However, ν_{12} and ν_{21} are not frequency-dependent; these two Poisson's ratios only depend on the geometric dimensions of a honeycomb cell. It is noteworthy that the proposed expressions of E_1, E_2 and G_{12} for the undamped case converge to the closed-form solution provided by Gibson and Ashby when the frequency parameter (ω) tends to zero as shown in the following paragraphs.

To understand the frequency-dependent behaviour of E_1, E_2 and G_{12}, we expand the expressions by a Taylor series in the frequency parameter ω. The only frequency-dependent term in E_1 and E_2 is D_{33}. Therefore, expanding D_{33} we have

$$D_{33} = \frac{EIb^3(\cos(bl)\sinh(bl) + \cosh(bl)\sin(bl))}{1 - \cos(bl)\cosh(bl)}$$

$$= 12\frac{EI}{l^3} + \left(\frac{13}{35}\,il\zeta_m m\right)\omega + \left(\frac{59}{161700}\,\frac{l^5\zeta_m^2 m^2}{EI} + \frac{13}{35}\,l\zeta_m m\,\zeta_k - \frac{13}{35}\,lm\right)\omega^2$$

$$+ \left(-\frac{59}{80850}\,\frac{il^5\zeta_m^2 m^2\zeta_k}{EI} + \frac{13}{35}\,ilm\,\zeta_k + \frac{59}{80850}\,\frac{il^5\zeta_m m^2}{EI} - \frac{551}{794593800}\,\frac{il^9\zeta_m^3 m^3}{EI^2} - \frac{13}{35}\,il\zeta_m m\,\zeta_k^2\right)\omega^3 + \cdots$$

$$\tag{13}$$

stiffness contribution, while the mass contribution is embedded in the parameter b (refer to equation (4)). The developed expressions are capable of providing a compound effect as well as individual effect of these parameters efficiently in a dynamic environment.

2.2.1. Remark 1: Poisson's ratios

The expressions of the two Poisson's ratios obtained in the preceding sections are not dependent on frequency and damping parameters; these expressions become same as the closed-form solution provided in literature [17]. The proposed expressions of the frequency dependent elastic moduli also conform the reciprocal theorem

$$E_1(\omega)\nu_{21} = E_2(\omega)\nu_{12} = \frac{Et^3(cS + Cs)b^3}{12\sin\theta\cos\theta(-1 + cC)} \tag{12}$$

where $C = \cosh(bl)$, $c = \cos(bl)$, $S = \sinh(bl)$ and $s = \sin(bl)$.

Considering the static case, that is, when the frequency $\omega \to 0$, from the above expansion we have

$$\lim_{\omega\to 0} D_{33} = 12\frac{EI}{l^3} = 12\left(\frac{1}{12}E\overline{b}t^3\right)\frac{1}{l^3} = E\overline{b}\left(\frac{t}{l}\right)^3 \tag{14}$$

Substituting this in the expressions of $E_1(\omega)$ and $E_2(\omega)$ in equations (7) and (8) we have

$$\lim_{\omega\to 0} E_1(\omega) = \frac{l\cos\theta}{(h+l\sin\theta)\overline{b}\sin^2\theta}\lim_{\omega\to 0}D_{33}$$

$$= E\left(\frac{t}{l}\right)^3\frac{l\cos\theta}{(h+l\sin\theta)\sin^2\theta} \tag{15}$$

and

$$\lim_{\omega \to 0} E_2(\omega) = \frac{(h + l \sin \theta)}{\bar{l}\bar{b}\cos^3 \theta} \lim_{\omega \to 0} D_{33} = E\left(\frac{t}{l}\right)^3 \frac{(h + l \sin \theta)}{\cos^3 \theta} \qquad (16)$$

The above expression match exactly with the original expressions of E_1 and E_2 presented in well-accepted literature [17] (refer to equations 25–26 of the supplementary material). The shear modulus $G_{12}(\omega)$ given in (9) is a function of four dynamic stiffness coefficients. In the limiting case they become

$$\lim_{\omega \to 0} D_{43}^s = -6\frac{EI}{l^2}, \quad \lim_{\omega \to 0} D_{33}^v = 96\frac{EI}{h^3},$$
$$\lim_{\omega \to 0} D_{34}^v = -24\frac{EI}{h^2} \quad \text{and} \quad \lim_{\omega \to 0} D_{44}^v = 8\frac{EI}{h} \qquad (17)$$

Substituting these in (9) we have

numerical results are presented for a structural configuration of $\theta = 30°$ and $h/l = 1$, with $\zeta_k = 0.002$ and $\zeta_m = 0.05$ (resulting in $b^4 = \frac{m\omega^2(1-i\omega/20)}{EI(1+i\omega/500)}$). The geometric parameters of the honeycomb and intrinsic material properties are assumed as: $l = 3.67$ mm, $h = l$, $E = 69.5 \times 10^3$ N/mm^2, $d = 0.8$ mm, $t = 0.0635$ mm and $m = 0.137$ kg/mm. The upper peaks in Fig. 3(a) are related to anti-resonance frequencies of the beam and Fig. 3(b) shows the corresponding phase-shift.

To verify the validity of the derived expression of the dynamic stiffness matrix we compare the results with the conventional finite element method considering a single beam element first. In Fig. 4(a) the responses of a pinned-pinned beam under the application of unit moment at the right edge are shown, wherein the rotational responses (radian) at the left and right edge are compared. The finite element results are obtained by discretising the beam into 100 elements and taking first 20 modes in the

$$\lim_{\omega \to 0} G_{12}(\omega) = \frac{(h + l \sin \theta)}{2l\bar{b}\cos \theta} \lim_{\omega \to 0} \frac{1}{\left(-\dfrac{h^2}{4lD_{43}^s} + \dfrac{2}{\left(D_{33}^v - \dfrac{(D_{34}^v)^2}{D_{44}^v} \right)} \right)}$$

$$= \frac{(h + l \sin \theta)}{2l\bar{b}\cos \theta} \frac{1}{\left(-\dfrac{h^2}{4l\left(-6\dfrac{EI}{l^2} \right)} + \dfrac{2}{\left(96\dfrac{EI}{h^3} - \dfrac{\left(-24\dfrac{EI}{h^2} \right)^2}{8\dfrac{EI}{h}} \right)} \right)} \qquad (18)$$

$$= E\left(\frac{t}{l}\right)^3 \frac{\left(\dfrac{h}{l} + \sin\theta\right)}{\left(\dfrac{h}{l}\right)^2 \left(1 + 2\dfrac{h}{l}\right)\cos\theta}$$

This shows that the shear modulus $G_{12}(\omega)$ given in equation (9), in the static limit, also reduces to the classical equation 29 [17] of the supplementary material. The expressions derived here can be viewed as a dynamic generalisation of the conventional equivalent elastic moduli of the hexagonal cellular forms.

3. Numerical illustrations

3.1. Dynamic stiffness elements

We first study the elements of the dynamic stiffness matrix as they appear directly in the expressions for the equivalent elastic moduli of hexagonal lattice metamaterials. The expressions of frequency dependent complex elastic moduli of the entire lattice are either directly dependent on a single dynamic stiffness element or the compound effect of multiple dynamic stiffness elements. Fig. 3 shows the variation of amplitude and phase of the complex dynamic stiffness elements with frequency (refer to Equation (6)). There are six unique dynamic stiffness elements, which are shown in this figure. The results are obtained directly from Equation (3) for a frequency value up to 200 rad/s. Unless otherwise mentioned,

response calculations. The dynamic stiffness results are obtained using the closed-form expression obtained from only one element. The results match very well, confirming the validity and efficiency of applying the dynamic stiffness method.

3.2. Dynamic elastic moduli of the lattice

In this subsection numerical results are presented for the frequency dependent in-plane elastic moduli (E_1, E_2 and G_{12}) of hexagonal cellular metamaterials based on the proposed formulae; the two Poisson's ratios (ν_{12} and ν_{21}) are not dependent on vibration characteristics of the structure. After establishing that a single beam element using the dynamic stiffness matrix is capable to capture the high-frequency dynamics (Fig. 4(a)), we have written a bespoke finite element code for the honeycomb lattice structure, where the element stiffness matrices of the constituting beams are replaced by the dynamic stiffness matrix. The finite element approach involves transforming the element dynamic stiffness matrices for all beam elements into the global coordinate system, assembling them and applying the boundary conditions. The finite element code of hexagonal honeycombs is validated for zero
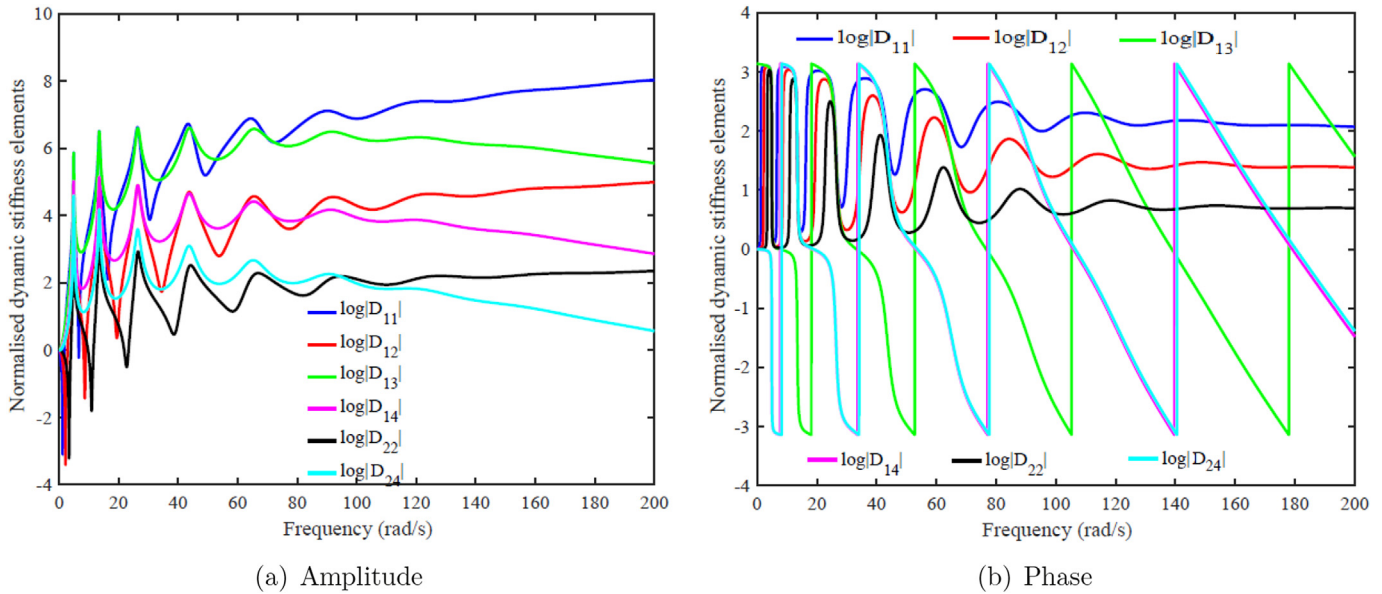
(a) Amplitude (b) Phase

Fig. 3. (a–b) The amplitude and phase of the frequency-dependent dynamic stiffness elements of a single beam (refer to Equation (3)). The elements of the dynamic stiffness matrix are presented in a normalised form with respect to the corresponding static stiffness matrix.

frequencies with the results obtained from the closed-form solutions provided by Gibson and Ashby [17] as shown in Table 1. The proposed analytical formulae for hexagonal lattices (under vibration) are validated using results obtained from the finite element code of hexagonal honeycombs. Fig. 4(b–c) shows the representative results obtained from the proposed closed-form expression for the frequency dependent Young's modulus along with the results generated using finite element simulations. For this study the results from the direct finite element approach involves the inversion of the global dynamic stiffness matrix of dimension 15042 × 15042. Numerical results obtained using this approach for every frequency value is compared with the closed-form analytical expressions derived in the paper. Two different configurations of regular honeycombs are considered with cell angle $\theta = 30°$ and the h/l ratio of 1 and 1.5. Minor difference in the numerical values of the two results corresponding to a wide range of frequency corroborates the validity of the proposed expressions. It can be noted that a conventional finite element method would require a very fine discretization of each of the constituent beams to capture the high-frequency dynamics. This will essentially make the structural matrices computationally unmanageable for a lattice structure having a high number of such beams. For this reason we have used an efficient dynamic stiffness based finite element method in this paper. The geometry, node numbers and nodal connectivity of the static case remains the same for the dynamic case. Therefore, the current validation along with the dynamic validation for a single beam ensures the validation for the dynamic responses of the entire lattice. The values of the elastic moduli amplifies considerably with increasing values of frequencies. Similar trend has been reported in literature for randomly parametrized beams [35]. The frequency values corresponding to the lower peaks of the curves for three frequency dependent elastic moduli can be regarded as the natural frequencies (analogous to the physical behaviour of resonance).

The effect of variation in the structural configuration of the hexagonal lattices is studied considering the h/l ratio and cell angle. Fig. 5(a − c) shows the effect of variation in the h/l ratio, while

Fig. 5(d − f) presents the effect of variation in the cell angle θ for the three frequency dependent elastic moduli. It can be observed that the numerical values of E_1 and G_{12} decrease with increment in the value of h/l, while a reverse trend is noticed for E_2. Unlike E_1 and E_2, the trend of the curves for G_{12} changes considerably with the variation of h/l ratio resulting a significant shift of the natural frequencies. The numerical value of E_1 decreases with increment in the value of cell angle θ, while a reverse trend is noticed for E_2 and G_{12}. Trends of the frequency-dependent elastic moduli with respect to h/l ratio and θ could be explained form the closed-form expressions presented in equations (7)–(9). The relationships are not readily evident through visual inspection of these equations containing coupled terms. However, the relationship of the elastic moduli with h/l ratio and θ can be easily explained in the static limit, that shows a similar nature (refer to equations 25−29 of the supplementary material). The trend of the curves representing the frequency dependent elastic moduli remain same implying no shift in the corresponding natural frequencies.

Fig. 6 presents the effect of variation of mass and stiffness proportional damping factors on the frequency dependent elastic moduli. The effect of variation in mass proportional damping factor is not found to be quite significant. It is observed that the difference between the upper and lower peak values of the elastic moduli increases marginally with the increase of mass proportional damping factor in the lower frequency range. The effect of variation of mass proportional damping becomes negligible in the higher frequency range. However, an opposite trend is noticed in case of the stiffness proportional damping factor, wherein the difference between the upper and lower peak values of the elastic moduli reduces significantly with the increase in stiffness proportional damping factor for the lower frequency range. In the higher frequency range, it is observed that the numerical values of the elastic moduli reduce with the increase in stiffness proportional damping factor.
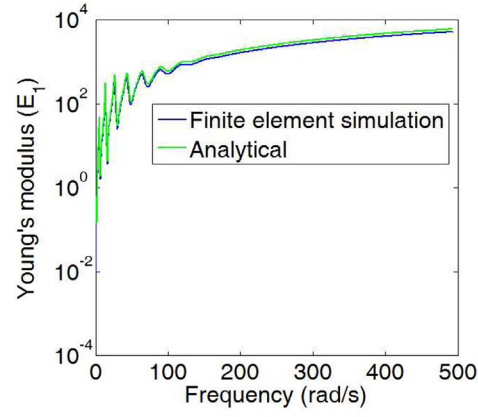
The mass and stiffness proportional damping factors are often important parameters to modulate the phase of the complex frequency dependent elastic moduli. Fig. 7 presents the effect of
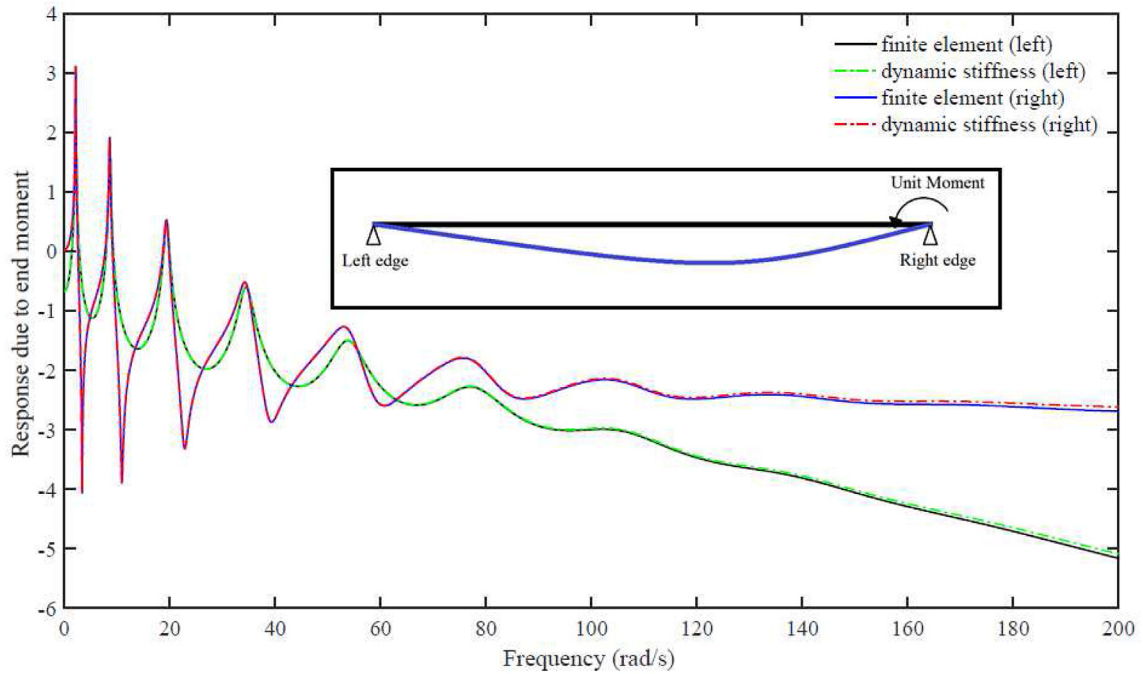
(a) Responses of a pinned-pinned beam
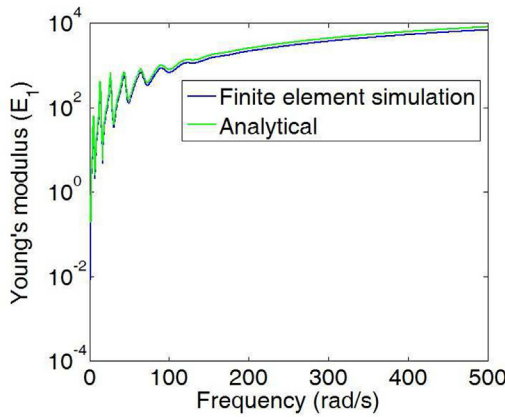
(b) $E_1 \ (h/l = 1)$

(c) $E_1 \ (h/l = 1.5)$

Fig. 4. (a) Frequency-dependent responses of a pinned-pinned beam under the application of a unit moment at the right edge (b–c) Frequency dependent Young's modulus (with $h/l = 1$ and $h/l = 1.5$) of hexagonal lattices with $\theta = 30°$ and $\zeta_m = 0.05$ and $\zeta_k = 0.002$.

Table 1
Validation of the finite element code for results obtained corresponding to static state with respect to the numerical values obtained from literature [17]. The results are presented as a ratio of the numerical values obtained using the finite element code (E_{1FE}, E_{2FE} and G_{12FE}) and the formulae provided by Gibson and Ashby (E_{1GA}, E_{2GA} and G_{12GA}).

Cell angle (θ)	$\dfrac{h}{l}$	$\dfrac{E_{1FE}}{E_{1GA}}$	$\dfrac{E_{2FE}}{E_{2GA}}$	$\dfrac{G_{12FE}}{G_{12GA}}$
30°	1	1.0012	1.0023	1.0051
30°	1.5	1.0021	1.0030	1.0046
45°	1	1.0028	1.0041	1.0037
45°	1.5	1.0017	1.0035	1.0052

variation of mass and stiffness proportional damping factors on the frequency dependent phases of the elastic moduli. From the closed-form expressions of the two complex Young's moduli (refer to Equations (7) and (8) for E_1 and E_2, respectively), it can be discerned that the expression of frequency dependent phase would be same for E_1 and E_2. For this reason, the effect of variation in mass and stiffness proportional damping are shown in a single figure for E_1 and E_2, while separate figures are furnished for G_{12}. In case of stiffness proportional damping, the difference between the upper and lower peak values of the phase values reduces significantly with the increase in stiffness proportional damping factor for the lower frequency range, while the effect is found to be much lesser for mass proportional damping. In the higher frequency range, it is observed that the numerical values of the phases reduce with the increase of the stiffness proportional damping factor. A phase-shift is noticed from positive to negative numerical values in case of G_{12}. The presented results reveal that the interesting attribute of phase-shift, that occurs in particular frequencies, can be further modulated by changing the mass and stiffness proportional damping factors according to application-specific requirements.

From the derivation of the elastic moduli (refer to subsection 2.1), it can be discerned that the Young's moduli E_1 and E_2 depend on the complex dynamic stiffness element D_{33} of a single
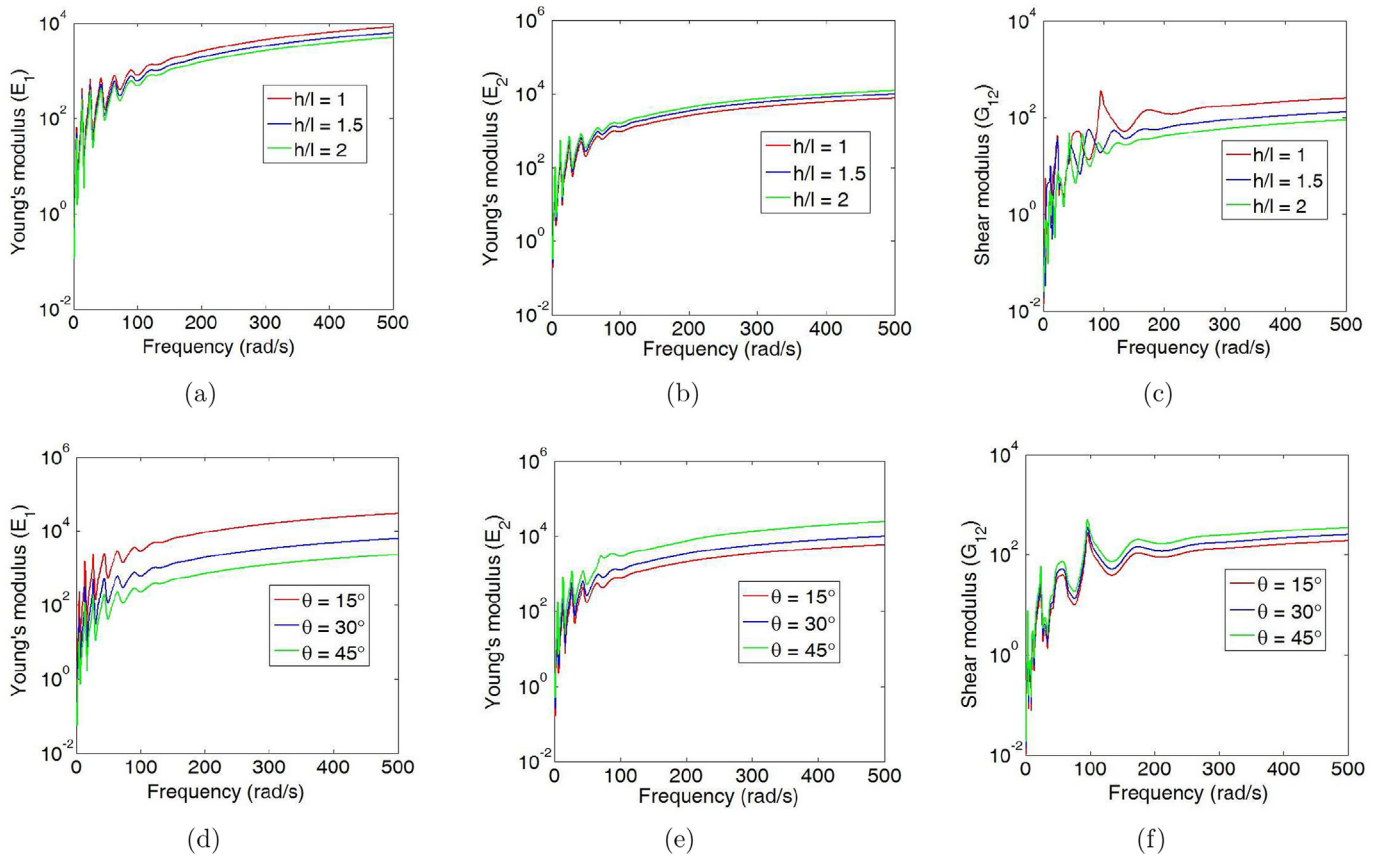
Fig. 5. (a–c) Frequency dependent normalised Young's moduli (E_1, E_2) and the shear modulus (G_{12}) of hexagonal lattices for different h/l ratios (d–f) Variation of frequency dependent normalised Young's moduli (E_1, E_2) and the shear modulus (G_{12}) of hexagonal lattices with cell angle θ

beam element only, while the shear modulus G_{12} depends on multiple dynamic stiffness elements of various beam elements. Thus, the results for the frequency-dependent amplitude of E_1 and E_2 show a similar trend as D_{33} with some constant multiplication factor depending on the structural geometry of the lattice, while the phase of E_1 and E_2 are exactly same as that of D_{33} (refer to Fig. 3). However, the amplitude and phase of G_{12} show a mixed effect resulting from multiple dynamic stiffness elements of multiple beam elements.

To derive the analytical formulae, we have used the Euler−Bernoulli beam formulation for simplicity. The Timoshenko beam theory can be used in future investigations that would obtain better results for the higher frequencies in comparison to the "exact" finite element simulations, but at the cost of more complex expressions. It can be noted in this context that the validation with the "exact" finite element method is given in this article at the element level considering single beams (refer to Fig. 3(c)), which shows a perfect agreement between the dynamic stiffness method and exact finite element method. The dynamic stiffness based approach, which is a high fidelity approach compared to the conventional "static" finite element method, is employed to obtain results for the lattice structure leading to significant amount of computational efficiency. The conventional "static" finite element method could require very fine discretization for higher frequencies that may be practically impossible to achieve in a complex lattice metamaterial.

4. Summary and perspective

The present article sheds light on two novel aspects related to

hexagonal lattices: the dependence of elastic moduli on frequencies and the nature of the complex valued elastic moduli.

It is observed that the amplitude of elastic moduli increase significantly with the increase in frequencies of a vibrating structure. This, in turn, indicates the necessity of considering the frequency dependence of elastic moduli in subsequent analysis and design of such structural elements where a dynamic effect is anticipated. The fundamental fact that natural frequency of a system is dependent on the elastic moduli led to this investigation, which addresses a logical reverse derivation that the elastic moduli should also be dependent on frequencies.

For the convenience of readers, the derived expressions for the frequency-dependent elastic moduli of hexagonal lattices are listed in Table 2. It can be noted that the in-plane Poisson's ratios (Equations (10) and (11)) are not dependent on frequency and the expressions are same as the case of static deformation provided in literature 17. The analytical formulae for frequency dependent elastic moduli reduce to the traditional static expressions provided by Gibson and Ashby [17] in case of the frequency tending towards zero. An interesting physical inference can be drawn from this observation relating the behaviour to the wavelength of vibrating frequency. The influence of vibrating frequency becomes significant in case of sub-wavelengths, while the effect of vibrating frequency on the elastic moduli reduces with the increase in wave lengths. The influence becomes equal to zero in the limiting case of very high wave length, which corresponds to purely static analysis of the lattice.

From a different viewpoint, the frequency dependence of elastic moduli in vibrating structures can be perceived advantageous in some instances and attempts could be made to exploit this effect in
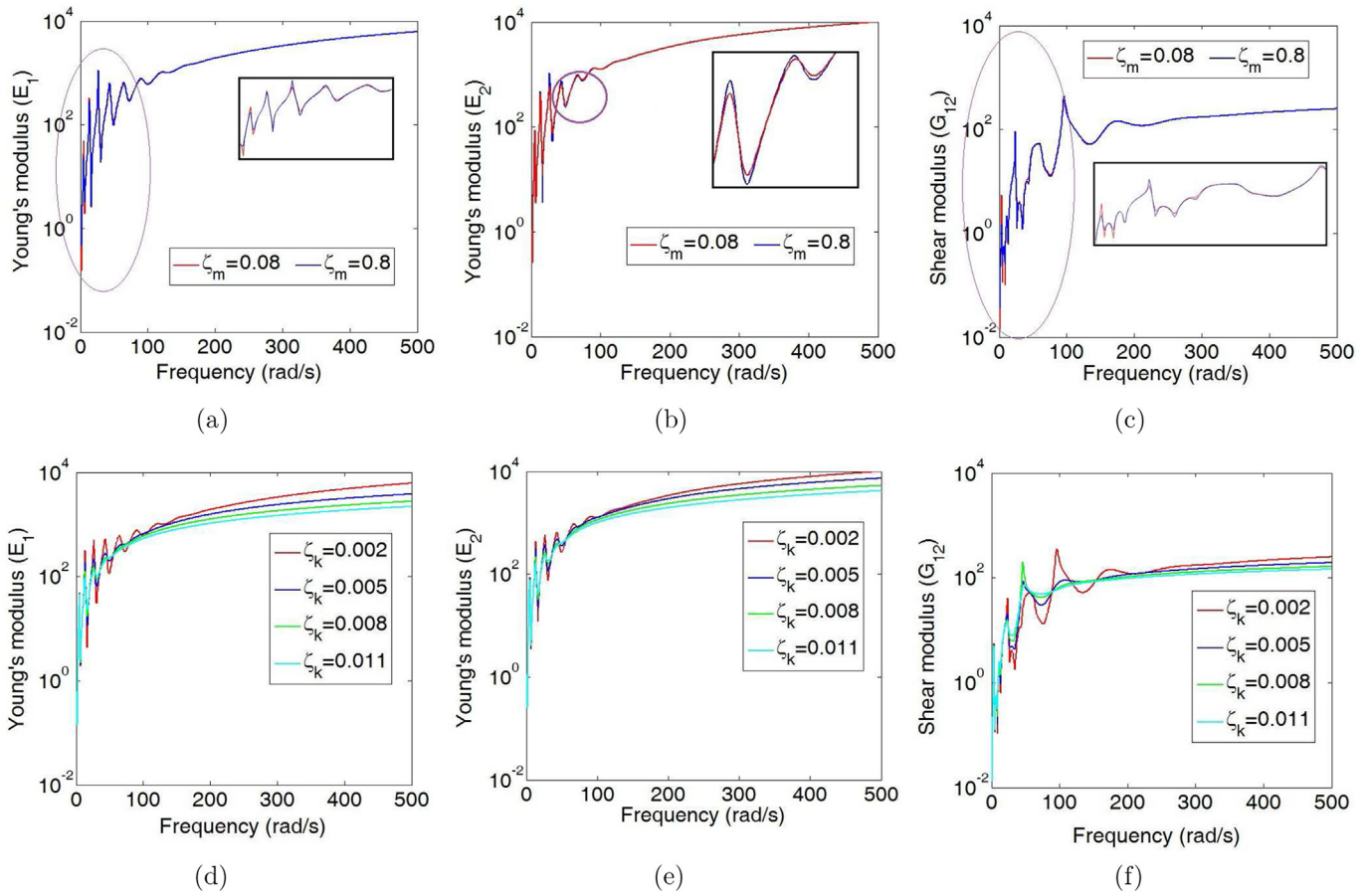
Fig. 6. (a–c) Effect of variation in mass proportional damping factor on normalised Young's moduli (E_1, E_2) and the shear modulus (G_{12}) (d–f) Effect of variation in stiffness proportional damping factor on normalised Young's moduli (E_1, E_2) and the shear modulus (G_{12}).

future investigations. For example, wind turbine blades or aerospace structures normally experience different ranges of vibration during the operating conditions. This essentially means that the frequency-dependent elastic moduli of the structural materials would have higher values than the conventional static counterparts, for which the structures are designed as per the current design practice. During the operating conditions, it perfectly makes sense to have higher values of the elastic moduli for wind turbine blades or aircraft wings that need to sustain a high value of wind load. Thus an increased value of the Young's moduli during the operating condition would reduce the deformations of such structures. Similar advantages can be achieved in various nano-mechanical devices, which often experience ambient vibration. Future attempts could be made to exploit these increased values of elastic moduli under a vibrating environment in the operating conditions for various engineering systems across the length-scales (nano to macro). Besides that, the analysis presented in this article shows that the natural frequencies of the lattice structure can be identified based on the plots of frequency dependent elastic moduli.

5. Conclusion

An analytical approach leading to closed-form expressions involving transcendental functions is presented for the frequency dependence of complex elastic moduli of cellular materials. The frequency-dependent dynamic stiffness matrix for a single damped beam element is developed first, followed by the derivation of expressions for the elastic moduli of the entire lattice structure based on analysing a unit cell. The expressions of elastic moduli involving transcendental functions derived here can be viewed as a dynamic generalisation of the well-known classical static elastic moduli. From the derived expressions it is observed that E_1, E_2 and G_{12} are functions of frequency, damping parameters, geometric dimensions of the hexagonal lattice and the intrinsic material property of the material. However, ν_{12} and ν_{21} are not frequency-dependent; these two moduli only depend on the geometric dimensions of a honeycomb cell. Numerical results for the two Young's moduli and shear modulus are presented to investigate the effect of variation in the excitation frequency on cellular materials. The frequency dependence of elastic moduli in vibrating structures can be perceived to be advantageous in various instances and attempts could be made to exploit this effect in future engineering applications leading to dramatic consequences in the conventional design practices. The developed expressions of elastic moduli exactly reduce to the standard formulae for hexagonal honeycombs when the driving frequency is set to zero (static deformation).

Although the focus has been on hexagonal lattices in this paper, the disseminated concepts can be extended to other forms of lattices and metamaterials. This investigation introduces the scope of including two crucial parameters (frequency dependence and damping constants) in the development of lattice metamaterials for vibrating structures, adding new dimensions in the field of metamaterials research. Along with different geometric attributes and intrinsic elastic modulus, the damping factors can be exploited to modulate the amplitude and phase of vibrating metamaterials
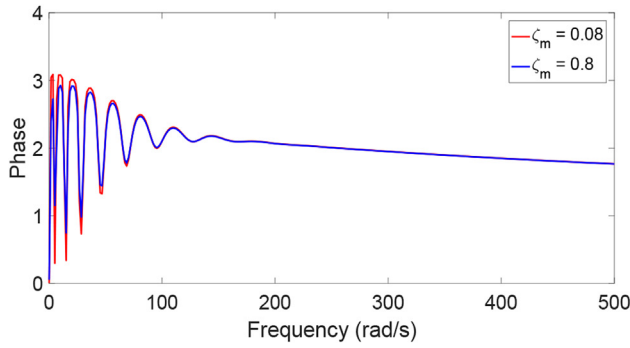
(a) Young's moduli E_1, E_2
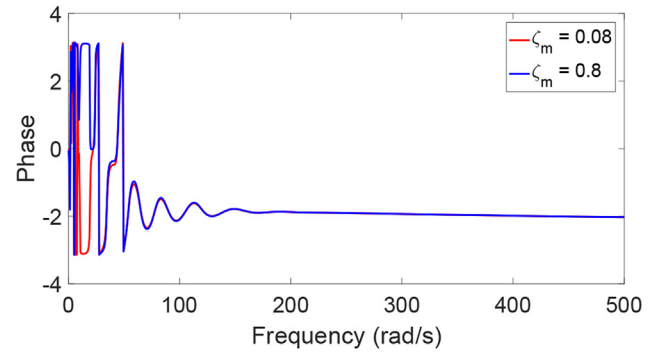
(b) Shear modulus G_{12}
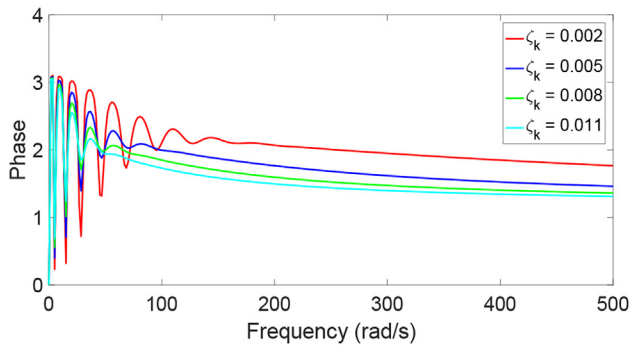
(c) Young's moduli E_1, E_2
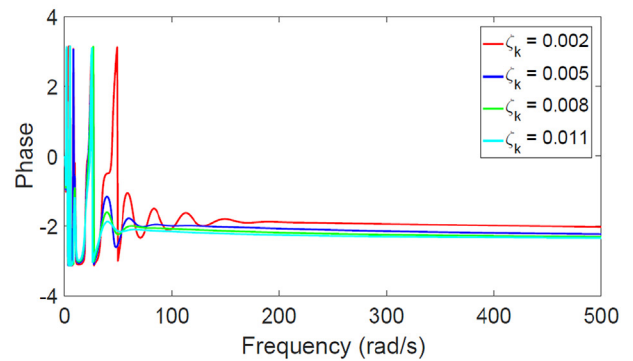
(d) Shear modulus G_{12}

Fig. 7. (a–b) Effect of variation in mass proportional damping factor on the phase of two Young's moduli (E_1 and E_2) and the shear modulus (G_{12}) (c–d) Effect of variation in stiffness proportional damping factor on the phase of two Young's moduli (E_1 and E_2) and the shear modulus (G_{12}).

Table 2

Summary of the formulae for effective frequency-dependent elastic moduli (E_1, E_2 and G_{12}) of hexagonal lattices (the in-plane Poisson's ratios are not dependent on frequency).

Here $b^4 = \dfrac{m\omega^2 - i\omega c_2}{EI + i\omega c_1}$, $i = \sqrt{-1}$, EI is the bending rigidity, m is mass per unit length, c_1 is the strain-rate-dependent viscous damping coefficient, c_2 is the velocity-dependent viscous damping coefficient, t is the thickness of honeycomb wall, h, l and θ are the length of cell walls and cell angle as shown in Fig. 1(b).

Elastic modulus	Generalised (complex valued) frequency-dependent expression	Classical expression ($\omega \to 0$)
$E_1(\omega)$	$\dfrac{Et^3 l \cos\theta\, b^3 (\cos(bl)\sinh(bl) + \cosh(bl)\sin(bl))}{12(h + l\sin\theta)\sin^2\theta(1 - \cos(bl)\cosh(bl))}$	$\dfrac{Et^3 \cos\theta}{l^2(h + l\sin\theta)\sin^2\theta}$
$E_2(\omega)$	$\dfrac{Et^3 (h + l\sin\theta)\, b^3 (\cos(bl)\sinh(bl) + \cosh(bl)\sin(bl))}{12\cos^3\theta(1 - \cos(bl)\cosh(bl))}$	$\dfrac{Et^3 (h + l\sin\theta)}{l^4 \cos^3\theta}$
$G_{12}(\omega)$	$\dfrac{Et^3 (h + l\sin\theta)\, b^3 \sin(bl)\sinh(bl)(1 + \cos(bh/2)\cosh(bh/2))}{6l\cos\theta\left[h^2 b(1 - \cos(bl)\cosh(bl))(1 + \cos(bh/2)\cosh(bh/2)) + 8l\sin(bl)\sinh(bl)(\cosh(bh/2)\sin(bh/2) - \sinh(bh/2)\cos(bh/2))\right]}$	$\dfrac{Et^3 (h + l\sin\theta)}{lh^2 (2h + l)\cos\theta}$

further. The insightful closed-form analytical expressions provide a computationally efficient way to investigate the problem in more detail. Such an efficient analytical approach can be particularly appealing in the development of application-specific material micro-structures where multiple realizations are needed to be performed due to involvement of inverse identification process based on optimization.

Appendix A. Supplementary data

Supplementary data to this article can be found online at https://doi.org/10.1016/j.actamat.2018.11.012.

References

[1] T. Allen, T. Hewage, C. Newton-Mann, W. Wang, O. Duncan, A. Alderson, Fabrication of auxetic foam sheets for sports applications, Phys. Status Solidi 254 (12) (2017), 1700596.

[2] A. Amendola, G. Carpentieri, L. Feo, F. Fraternali, Bending dominated response of layered mechanical metamaterials alternating pentamode lattices and confinement plates, Compos. Struct. 157 (2016) 71–77.

[3] J.R. Banerjee, Dynamic stiffness formulation for structural elements: a general

approach, Comput. Struct. 63 (1) (1997) 101–103.

[4] Y. Chen, M. Barnhart, J. Chen, G. Hu, C. Sun, G. Huang, Dissipative elastic metamaterials for broadband wave mitigation at subwavelength scale, Compos. Struct. 136 (2016) 358–371.

[5] Y. Chen, Z. Jia, L. Wang, Hierarchical honeycomb lattice metamaterials with improved thermal resistance and mechanical properties, Compos. Struct. 152 (2016) 395–402.

[6] J. Christensen, M. Kadic, O. Kraft, M. Wegener, Vibrant times for mechanical metamaterials 5 (3) (2015) 453–462.

[7] Y. Ding, Z. Liu, C. Qiu, J. Shi, Metamaterial with simultaneously negative bulk modulus and mass density, Phys. Rev. Lett. 99 (2007), 093904.

[8] H.-W. Dong, S.-D. Zhao, Y.-S. Wang, C. Zhang, Topology optimization of anisotropic broadband double-negative elastic metamaterials, J. Mech. Phys. Solid. 105 (2017) 54–80.

[9] J.F. Doyle, Wave Propagation in Structures, Springer Verlag, New York, 1989.

[10] O. Duncan, T. Allen, L. Foster, T. Senior, A. Alderson, Fabrication, characterisation and modelling of uniform and gradient auxetic foam sheets, Acta Mater. 126 (2017) 426–437.

[11] F.K.A. El-Sayed, R. Jones, I.W. Burgess, A theoretical approach to the deformation of honeycomb based composite materials, Composites 10 (4) (1979) 209–214.

[12] N. Fang, D. Xi, J. Xu, M. Ambati, W. Srituravanich, C. Sun, X. Zhang, Ultrasonic metamaterials with negative modulus, Nat. Mater. 5 (6) (06 2006) 452–456.

[13] C. Findeisen, J. Hohe, M. Kadic, P. Gumbsch, Characteristics of mechanical metamaterials based on buckling elements, J. Mech. Phys. Solid. 102 (2017) 151–164.

[14] N.A. Fleck, V.S. Deshpande, M.F. Ashby, Micro-architectured materials: past, present and future, Proc. Roy. Soc. Lond.: Math. Phys. Eng. Sci. 466 (2121) (2010) 2495–2516.

[15] R. Fleury, D.L. Sounas, C.F. Sieck, M.R. Haberman, A. Alù, Sound isolation and giant linear nonreciprocity in a compact acoustic circulator, Science 343 (6170) (2014) 516–519.

[16] E.S. Flores, F. DiazDelaO, M. Friswell, J. Sienz, A computational multi-scale approach for the stochastic mechanical response of foam-filled honeycomb cores, Compos. Struct. 94 (5) (2012) 1861–1870.

[17] L. Gibson, M.F. Ashby, Cellular Solids Structure and Properties, Cambridge University Press, Cambridge, UK, 1999.

[18] J.N. Grima, L. Mizzi, K.M. Azzopardi, R. Gatt, Auxetic perforated mechanical metamaterials with randomly oriented cuts, Adv. Mater. 28 (2) (2016) 385–389.

[19] T.A.M. Hewage, K.L. Alderson, A. Alderson, F. Scarpa, Double-negative mechanical metamaterials displaying simultaneous negative stiffness and negative Poisson's ratio properties, Adv. Mater. 28 (46) (2016) 10323–10332.

[20] H. Huang, C. Sun, Locally resonant acoustic metamaterials with 2D anisotropic effective mass density, Phil. Mag. 91 (6) (2011) 981–996.

[21] M.I. Hussein, M.J. Leamy, M. Ruzzene, Dynamics of phononic materials and structures: historical origins, recent progress, and future outlook, Appl. Mech. Rev. 66 (4) (05 2014), 040802–040838.

[22] S. Janbaz, R. Hedayati, A.A. Zadpoor, Programming the shape-shifting of flat soft matter: from self-rolling/self-twisting materials to self-folding origami, Mater. Horiz. 3 (2016) 536–547.

[23] W.Y. Jang, S. Kyriakides, On the buckling and crushing of expanded honeycomb, Int. J. Mech. Sci. 91 (2015) 81–90.

[24] M. Kadic, T. Buckmann, N. Stenger, M. Thiel, M. Wegener, On the practicability of pentamode mechanical metamaterials, Appl. Phys. Lett. 100 (19) (2012) 1901.

[25] S. Khakalo, V. Balobanov, J. Niiranen, Modelling size-dependent bending, buckling and vibrations of 2d triangular lattices by strain gradient elasticity models: applications to sandwich beams and auxetics, Int. J. Eng. Sci. 127 (2018) 33–52.

[26] K. Kim, J. Ju, Mechanical metamaterials with 3d compliant porous structures, Compos. Struct. 132 (2015) 874–884.

[27] H.M.A. Kolken, S. Janbaz, S.M.A. Leeflang, K. Lietaert, H.H. Weinans, A.A. Zadpoor, Rationally designed meta-implants: a combination of auxetic and conventional meta-biomaterials, Mater. Horiz. 5 (2018) 28–35.

[28] K. Li, X.L. Gao, J. Wang, Dynamic crushing behavior of honeycomb structures with irregular cell shapes and non-uniform cell wall thickness, Int. J. Solid Struct. 44 (14–15) (2007) 5003–5026.

[29] T. Li, X. Hu, Y. Chen, L. Wang, Harnessing out-of-plane deformation to design 3d architected lattice metamaterials with tunable Poissons ratio, Sci. Rep. 7 (2017) 8949.

[30] X. Li, H. Gao, Mechanical metamaterials: smaller and stronger, Nat. Mater. 15 (4) (2016) 373–374.

[31] W. Liu, N. Wang, J. Huang, H. Zhong, The effect of irregularity, residual convex units and stresses on the effective mechanical properties of 2d auxetic cellular structure, Mater. Sci. Eng., A 609 (2014) 26–33.

[32] A. Mahata, T. Mukhopadhyay, Probing the chirality-dependent elastic properties and crack propagation behavior of single and bilayer stanene, Phys. Chem. Chem. Phys. 20 (2018) 22768–22782.

[33] S. Malek, L. Gibson, Effective elastic properties of periodic hexagonal honeycombs, Mech. Mater. 91 (1) (2015) 226–240.

[34] S. Malek, L.J. Gibson, Multi-scale modelling of elastic properties of balsa, Int. J. Solid Struct. 113–114 (2017) 118–131.

[35] C. Manohar, S. Adhikari, Dynamic stiffness of randomly parametered beams, Probabilist. Eng. Mech. 13 (1) (1998) 39–51.

[36] L.R. Meza, G.P. Phlipot, C.M. Portela, A. Maggi, L.C. Montemayor, A. Comella, D.M. Kochmann, J.R. Greer, Reexamining the mechanical property space of three-dimensional lattice architectures, Acta Mater. 140 (2017) 424–432.

[37] M.-A. Miri, E. Verhagen, A. Alù, Optomechanically induced spontaneous symmetry breaking, Phys. Rev. 95 (May 2017), 053822.

[38] M.B. Muhlestein, M.R. Haberman, A micromechanical approach for homogenization of elastic metamaterials with dynamic microstructure, Proc. Roy. Soc. Lond.: Math. Phys. Eng. Sci. 472 (2016) (2192).

[39] T. Mukhopadhyay, S. Adhikari, Effective in-plane elastic properties of auxetic honeycombs with spatial irregularity, Mech. Mater. 95 (2016) 204–222.

[40] T. Mukhopadhyay, S. Adhikari, Equivalent in-plane elastic properties of irregular honeycombs: an analytical approach, Int. J. Solid Struct. 91 (2016) 169–184.

[41] T. Mukhopadhyay, S. Adhikari, Free-vibration analysis of sandwich panels with randomly irregular honeycomb core, J. Eng. Mech. 142 (11) (2016), 06016008.

[42] T. Mukhopadhyay, S. Adhikari, Effective in-plane elastic moduli of quasi-random spatially irregular hexagonal lattices, Int. J. Eng. Sci. 119 (2017) 142–179.

[43] T. Mukhopadhyay, S. Adhikari, Stochastic mechanics of metamaterials, Compos. Struct. 162 (2017) 85–97.

[44] T. Mukhopadhyay, S. Adhikari, A. Batou, Frequency domain homogenization for the viscoelastic properties of spatially correlated quasi-periodic lattices, Int. J. Mech. Sci. (2017), https://doi.org/10.1016/j.ijmecsci.2017.09.004.

[45] T. Mukhopadhyay, A. Mahata, S. Adhikari, M. Asle Zaeem, Probing the shear modulus of two-dimensional multiplanar nanostructures and heterostructures, Nanoscale 10 (2018) 5280–5294.

[46] T. Mukhopadhyay, A. Mahata, S. Adhikari, M.A. Zaeem, Effective elastic properties of two dimensional multiplanar hexagonal nanostructures, 2D Mater. 4 (2) (2017), 025006.

[47] T. Mukhopadhyay, A. Mahata, S. Adhikari, M.A. Zaeem, Effective mechanical properties of multilayer nano-heterostructures, Sci. Rep. 7 (1) (2017) 15818.

[48] S.D. Papka, S. Kyriakides, In-plane compressive response and crushing of honeycomb, J. Mech. Phys. Solid. 42 (10) (1994) 1499–1532.

[49] S.D. Papka, S. Kyriakides, Experiments and full-scale numerical simulations of in-plane crushing of a honeycomb, Acta Mater. 46 (8) (1998) 2765–2776.

[50] M. Schaeffer, M. Ruzzene, Wave propagation in multistable magneto-elastic lattices, Int. J. Solid Struct. 56–57 (2015) 78–95.

[51] J.L. Silverberg, A.A. Evans, L. McLeod, R.C. Hayward, T. Hull, C.D. Santangelo, I. Cohen, Using origami design principles to fold reprogrammable mechanical metamaterials, Science 345 (6197) (2014) 647–650.

[52] A. Srivastava, Elastic metamaterials and dynamic homogenization: a review, Int. J. Soc. Netw. Min. 6 (1) (2015) 41–60.

[53] D. Torrent, J. Sanchez-Dehesa, Anisotropic mass density by two-dimensional acoustic metamaterials, New J. Phys. 10 (2) (2008), 023004.

[54] N. Triantafyllidis, M.W. Schraad, Onset of failure in aluminum honeycombs under general in-plane loading, J. Mech. Phys. Solid. 46 (6) (1998) 1089–1124.

[55] T. van Manen, S. Janbaz, A.A. Zadpoor, Programming 2d/3d shape-shifting with hobbyist 3d printers, Materials Horizons 4 (2017) 1064–1069.

[56] E. Vilchevskaya, I. Sevostianov, Effective elastic properties of a particulate composite with transversely-isotropic matrix, Int. J. Eng. Sci. 94 (2015) 139–149.

[57] A. Wilbert, W.Y. Jang, S. Kyriakides, J.F. Floccari, Buckling and progressive crushing of laterally loaded honeycomb, Int. J. Solid Struct. 48 (5) (2011) 803–816.

[58] H. Xu, A. Farag, D. Pasini, Multilevel hierarchy in bi-material lattices with high specific stiffness and unbounded thermal expansion, Acta Mater. 134 (2017) 155–166.

[59] Z. Yang, J. Mei, M. Yang, N.H. Chan, P. Sheng, Membrane-type acoustic metamaterial with negative dynamic mass, Phys. Rev. Lett. 101 (Nov 2008), 204301.

[60] A.A. Zadpoor, Mechanical meta-materials, Mater. Horiz. 3 (5) (2016) 371–381.

[61] J. Zhang, M.F. Ashby, The out-of-plane properties of honeycombs, Int. J. Mech. Sci. 34 (6) (1992) 475–489.

[62] X. Zheng, H. Lee, T.H. Weisgraber, M. Shusteff, J. DeOtte, E.B. Duoss, J.D. Kuntz, M.M. Biener, Q. Ge, J.A. Jackson, S.O. Kucheyev, N.X. Fang, C.M. Spadaccini, Ultralight, ultrastiff mechanical metamaterials, Science 344 (6190) (2014) 1373–1377.

[63] H. Zhu, Size-dependent elastic properties of micro- and nano-honeycombs, J. Mech. Phys. Solid. 58 (5) (2010) 696–709.

[64] C. Zschernack, M.A. Wadee, C. Vollmecke, Nonlinear buckling of fibre-reinforced unit cells of lattice materials, Compos. Struct. 136 (2016) 217–228.